J. Pure Appl. Ultrason. 35 (2013)pp. 125-128

Photoacoustic examination of red blood cell suspensions*

Ratan K. Saha, Subhajit Karmakar and Madhusudan Roy*

Saha Institute of Nuclear Physics,

1/AF Bidhannagar, Kolkata-700 064, W.B.

Email: ratank.saha@gmail.com

This study aims to investigate the role of red blood cell (RBC) concentration on photoacoustics (PAs). The time dependent PA signals from a collection of RBCs were simulated using a recently developed theoretical model. This model assumes each RBC as a fluid sphere and the PA signals from many cells are generated by adding the contributions from the individual cells. A Monte Carlo technique was implemented to generate the random locations of RBCs within a 2D simulation volume (200x200 μm^2) mimicking a tissue realization. The PA signals were simulated for the 355 and 532 nm irradiating optical radiations. Our simulation results demonstrated that PA signal amplitude increased monotonically with RBC concentration for both input radiations and exhibited similar trends with those of experiments. The experiments were conducted with porcine RBCs suspended in saline water. A Nd:YAG laser system was used to provide the desired radiation and the detection of acoustic signals were made by a needle hydrophone. Good agreement between theoretical and experimental results confirms the validity of the theoretical model.

Keywords: Red blood cells, Photoacoustics, 2D simulation.

Introduction

Since the discovery by Alexander Graham Bell in 1880 the photoacoustic (PA) effect finds many applications in a wide spectrum of biomedical sciences due to its superior imaging ability arising out of the fact that this technique combines high optical contrast and high spatial resolution due to modern advanced ultrasound transducer technology[1,2]. Besides, there is an increasing need for a noninvasive modality for monitoring of cerebral hemodynamics, electrical activity, and brain tissue oxygen tension or cerebral venous blood oxygenation (oxyhemoglobin saturation), specially, for patients of traumatic brain injuries in intensive care unit, and the photoacoustic modality may suitably be explored to meet such challenges. It is interesting to mention that functional photoacoustic microscopy, which provides multiwavelength imaging of optical absorption and permits high spatial resolution, detects absorbed photons ultrasonically through the photoacoustic effect[3]. When a short-pulsed laser irradiates biological tissues, wideband photoacoustic waves are induced as a result of transient thermoelastic expansion and the magnitude of the photoacoustic waves is proportional to the local optical energy deposition and, hence, the waves divulge physiologically specific optical absorption contrasts[4]. There are reports on characterization of various biomedical samples (e.g. cancer cells) based on photoacoustics signal[5, 6, 7]. Further, monitoring of blood oxygenation in human systems becomes an important issue among researchers[8, 9].

Recently, the present authors have also reported a work to assess blood oxygen saturation using photoacoustic technique and checked accuracy of the photoacoustic (PA) technique using two laser beams theoretically[10]. In this work a Monte Carlo technique was used to simulate 2D tissue configurations, and the PA signals from many red blood cells (RBCs) were constructed by summing the signals emitted by the individual cells. The level of oxygenation of each cell was assumed to be identical in a configuration. The cellular oxygenation state defined the blood SO_2 and also controlled the PA signal amplitude. Further, the authors presented a modeling approach to examine the dependence of the optoacoustic signals on blood oxygenation and explained that this approach is suitable to model the situations when the individual cells have the same oxygenation level in a blood sample[11].

In this paper the authors have undertaken to investigate the role of red blood cell (RBC) concentration on photoacoustics (PAs) and simulate the time dependent PA signals from a collection of RBCs using a recently developed theoretical model.

PA field calculation from blood:

A theoretical model has been developed recently to describe the PA field generated by a collection of cells approximated as fluid spheres suspended in

*This paper was conferred Dr.M. Pancholy Award for best presentation at National symposium on Ultrasonics, NSU-XIX, 30-31 Oct., 2012

*Life member Ultrasonics Society of India

another fluid medium. The PA field generated by a single spherical absorber has been obtained by solving a wave equation using the appropriate boundary conditions (*i.e.* continuity of pressure and normal component of particle velocity)[12]. The PA field for a uniformly illuminated ensemble of absorbers of identical size and under similar physical conditions can be calculated by summing the contributions from individual spheres as[13, 14],

$$p(\vec{r},\omega) = \frac{iI_0\mu_s\beta_s v_s a_s^2}{C_{Ps}}\phi_s \sum_{n=1}^{N} \frac{\exp\,(ik_f|\vec{r}-\vec{r_n}|)}{|\vec{r}-\vec{r_n}|}, \quad \ldots (1)$$

$$\phi_s = \frac{j_1(k_s a_s)\exp\,(-ik_f a_s)}{(1-\hat{\rho})\frac{\sin k_s a_s}{k_s a_s} - \cos k_s a_s + i\hat{\rho}\hat{v}\sin k_s a_s}, \quad \ldots (2)$$

with $\hat{\rho} = \rho_s/\rho_f$, $\hat{v} = v_s/v_f$, $k_s = \omega/v_s$ and $k_f = \omega/v_f$.

Here, I_0 is the intensity of the incident optical beam with modulation frequency ω; a_s is the radius of an absorbing sphere; β_s is the thermal expansion coefficient for the absorber; C_{Ps} is the isobaric heat capacity per unit mass for the absorbing region; μ_s is the optical absorption coefficient for the absorber; ρ_s is the density for the absorber; v_s is the speed of sound within the absorber; and $\overrightarrow{r_n}$ represents the position vector of the n[th] PA source. The density and speed of sound for the surrounding medium are indicated by ρ_f and v_f, respectively. The wave numbers inside and outside the absorber are denoted by k_s and k_f, respectively. The last term in Eq. (1) represents the interference of waves emitted by different absorbers. The PA geometry is shown in Fig. 1. The time domain pressure field can be obtained by taking the Fourier transform of Eq. (1) as[13, 14],

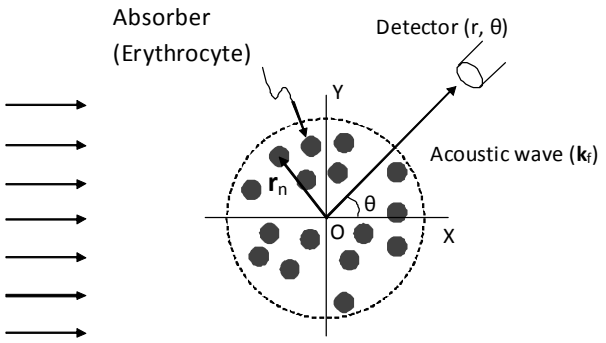

Fig.1: PA geomatry

$$p(\vec{r},t) \approx \frac{i\mu_s\beta_s v_s a_s^2 F}{2\pi r C_{Ps}} \int_{-\infty}^{\infty} d\omega\, \phi_s \exp\left[i\left(k_f r - \omega t\right)\right] \sum_{n=1}^{N} \exp\left(-i\overrightarrow{k_f}\cdot\overrightarrow{r_n}\right). \quad \ldots (2)$$

Here, F is the fluence of the optical radiation and N is the total number of absorbers present within the irradiated region. The notation $\overrightarrow{k_f}$ defines the direction of observation.

Materials and methods

Numerical simulation: The theoretical PA signal was obtained by computing Eq. (2). The integration was evaluated using the trapezoidal rule. Eq. (2) provided complex pressure at each time instant. The real part of the time series data provided the radio frequency line and the envelope was obtained using real and imaginary parts of those time series data. The density and compressibility of the surrounding medium was chosen as, $\rho_f = 1005$ kg/m^3 and $v_f = 1498$ m/s[15]. The density and compressibility for an erythrocyte were taken as $\rho_s = 1078$ kg/m^3 and $v_s = 1628$ m/s[15]. The thermal expansion coefficient and heat capacity per unit mass were selected as $\beta_s = 1.5 \times 10^{-4}$ K^{-1} and $C_{Ps} = 3.23 \times 10^3$ J kg^{-1} K^{-1} [16]. The optical absorption coefficient (μ_s) for an erythrocyte was estimated as 1089.63 and 465.82 cm^{-1} at 355 and 532 nm, respectively[17].

Eq. (2) was calculated for a collection of RBCs randomly distributed in a 2D region. The size of the 2D region was taken as 200x200 μm^2. This volume was occupied by the RBCs which were uniformly illuminated by the optical beam. A Monte Carlo algorithm known as the random sequential adsorption technique was implemented to generate the random locations of RBCs under non-overlapping condition[11-14]. Each cell in this study was approximated as a fluid sphere with radius $a_s = 2.53$ μm.

The theoretical PA signals were calculated with various blood samples with hematocrit varying from 10 to 50% at a step of 10% (hematocrit is referred to as the volume fraction occupied by RBCs in a blood sample). For each hematocrit, 100 RF lines were computed and the mean PA amplitude was evaluated.

Sample preparation: Fresh porcine blood was collected from a local slaughter house with EDTA (3 g/l). The whole blood was centrifuge at 3000 RPM for 30 min and successively the plasma and the buffy coat were removed gently. The packed cells were mixed with phosphate buffered saline (PBS) solution.

It is an isotonic solution that keeps the shapes of the cells intact. The mixture was centrifuged for 15 min at 3000 RPM to wash the RBCs. This step was repeated one more time for thorough washing of the cells. After washing, PBS was poured into the packed cells to achieve prepare samples having hematocrits between 10% to 50% at a step of 10%. The samples were stored overnight at 4^0 C and the experiments were performed on next day.

Experimental set up: A schematic diagram of the experimental set up is shown in Fig. 2. A Q-switched pulsed Nd:YAG laser (Quanta-Ray Lab-150, Spectra-Physics Inc., Santa Clara, CA) generating 20 ns pulses with 10 Hz repetition frequency was employed to irradiate the samples. The laser beam consists of three wavelengths (266, 355, 532 and 1064 nm). However, only one wavelength was selected at a time using a dichroic mirror (Edmund Optics, Singapore Pte. Ltd., Singapore). In this *in vitro* study, a blood sample was loaded in a rectangular glass cuvette (Optiglass, UK) and placed centrally within a water tank using a custom made sample holder. The laser beam entered the tank through an optical window mounted at its front surface as shown in the figure and illuminated the sample. A needle hydrophone (Precision Acoustics, UK) with 1 mm diameter was used to detect acoustic signals in the forward direction. The captured signals were displayed as well as recorded in a digital oscilloscope (TDS5034B, Tektronix Inc., Beaverton, OR). For each sample 100 such signals were recorded and mean peak amplitude corresponding to the illuminated surface was computed.

Results

The variation of theoretical mean PA signal amplitude corresponding to the illuminated surface of the sample is shown in Fig. 3(a) as a function of RBC volume concentration for 355 nm incident optical radiation. Each datum has been normalized by that of the 40% hematocrit. Normalized experimental results are also displayed is the same figure. It can be seen that theoretical trend is in excellent agreement with that of the experiment over the entire hematocrit range that has been studied in this work.

Fig. 3(b) demonstrates how the simulated average PA signal amplitude varies with RBC volume concentration when 532 nm optical radiation illuminates the sample. Associated normalized experimental results are also illustrated in the same figure. Note that small difference between theoretical and experimental curves is observed at lower hematocrit (i.e. <40%), however, the curves exhibit good agreement at higher hematocrit (i.e. > 40%).

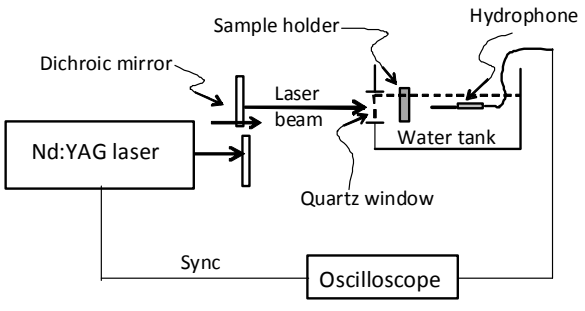

Fig. 2: Schematic diagram of experimental setup.

Discussion and conclusions

PAs of RBCs suspended in a saline solution (mimicking blood plasma) has been studied both theoretically and experimentally. The theoretical

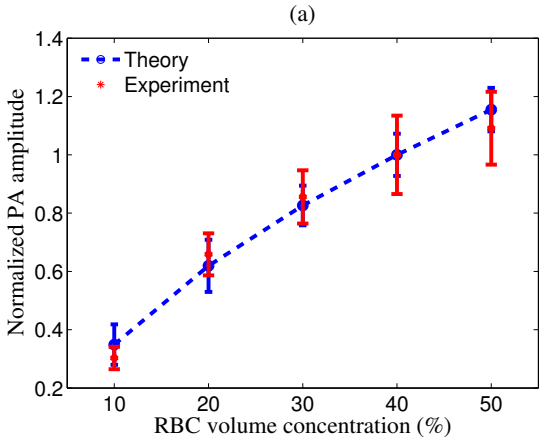

Fig. 3(a): Variation of PA amplitude with RBC concentration using 355nm radiation.

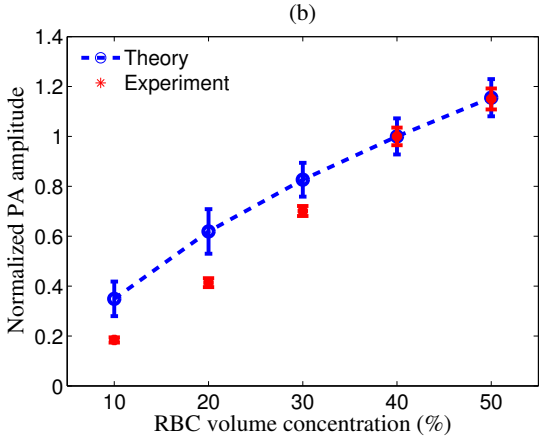

Fig. 3(b): Variation of PA amplitude with RBC concentration using 532nm radiation.

formulation relies on the single particle approach. That means PA field from a collection of cells has been obtained by summing the fields emitted by the individual cells. This approach works well for sparse medium and has been successfully utilized to interpret light and ultrasound scattering results. Recently PA experimental results have also been interpreted using this model.

Previously, Karpiouk *et.al*[18] conducted similar experiments and found that the PA amplitude increased as the concentration of RBCs increased. However, they did not compare the experimental results with that of theory. Our results are consistent with their published experimental results and that validates the experimental protocol adapted in this study. Additionally good agreement between the theoretical and experimental results confirms the validity of the theoretical model.

In conclusion, it is shown in this study that the PA amplitude monotonically increases with hematocrit for both optical radiations. The theoretical and the experimental results exhibit similar trends. This behaviour can be explained on the basis of the fact that as the hematocrit increases the number of PA sources adjacent to the illuminated surface also increases. Such an increase results in coherent addition of signals leading to the increase of PA amplitude. In future, it would be interesting to examine how the PA amplitude varies with hematocrit when RBCs are suspended in blood plasma. This would approximate the real blood more accurately and the knowledge of such experiments would help to develop the PA technique as a potential blood characterization tool.

Acknowledgements

The authors would like to thank Prof. Samita Basu and Prof. Abhijit Chakraborty of SNIP for providing their laboratory facility and their group members for constant support. We also like to thank Mr. Syamaprasad Mallik for assistance.

References

1 Duck F. A., *Physical Properties of Tissue*, Academic Press London (1990).

2 Wang L. V. and Hu S., Photoacoustic Tomography: In Vivo Imaging from Organelles to Organs, *Science*, 335 (2012) 1458-1462.

3 Sun T. and Diebold G. J., Generation of ultrasonic waves from a layered photoacoustic source, *Nature*, 355 (1992) 806–808.

4 Zhang H. F., Maslov K., Stoica G. and Wang L. V., Functional photoacoustic microscopy for high-resolution and noninvasive *in vivo* imaging, *Nat. Biotechnol.*, 24 (2006) 848-851.

5 Weight R. M., Viator J. A., Dale P S, Caldwell C W and Lisle A E, Photoacoustic detection of metastatic melanoma cells in the human circulatory system, *Opt. Lett.*, 31 (2006) 2998-3000.

6 Copland J. A., Eghtedari M., Popov V L, Kotov N, Mamedova N, Motamedi M and Oraevsky A A, Bioconjugated gold nanoparticles as a molecular based contrast agent: Implications for imaging of deep tumors using optoacoustic tomography, *Mol. Imaging Biol.*, 6 (2004) 341-349.

7 Eghtedari M., Motamedi M., Popov V. L., Kotov N. A. and Oraevsky A A, Optoacoustic imaging of gold nanoparticles targeted to breast cancer cells, *Proc. of SPIE*, 5320 (2004) 21-28.

8 Brecht H. P., Prough D. S., Petrov Y. Y., Patrikeev I., Petrova I. Y., Deyo D. J., Cicenaite I. and Esenaliev R. O., *In vivo* monitoring of blood oxygenation in large veins with a triple-wavelength optoacoustic system, *Opt. Express*, 15 (2007) 16261-16269.

9 Laufer J., Delpy D., Elwell C., and Beard P., Quantitative spatially resolved measurement of tissue chromophore concentrations using photoacoustic spectroscopy: application to the measurement of blood oxygenation and haemoglobin concentration, *Phys. Med. Biol*., 52 (2007) 141-168.

10 Saha R. K., Karmakar S. and Roy M., Assessment of blood oxygen saturation using photoacoustic technique, *J Opt , DOI* 10.1007/s12596 3 (2013) 013-0123.

11 Saha R. K., Karmakar S., Hysi E, Roy M and Kolios M C, Validity of a theoretical model to examine blood oxygenation dependent optoacoustics, *Journal of Biomedical Optics* 17(5), 055002 (2012).

12 Diebold G. J., Photoacoustic monopole radiation: Waves from objects with symmetry in one, two and three dimensions, in *Photoacoustic imaging and spectroscopy*, Edt. Wang L. V., Taylor and Francis Group, LLC, Chapter 1 (2009) 3-17.

13 Saha R. K. and Kolios M. C., A simulation study on photoacoustic signals from red blood cells, *J. Acoust. Soc. Am.*, 129 (2011) 2935-2943.

14 Saha R. K. and Kolios M. C., Effects of erythrocyte oxygenation on optoacoustic signals, *J. Biomed. Opt*., 16, (2011) 115003.

15 Shung K. K., Yuan Y. W., Fei D. Y. and Tarbell J. M., Effect of flow disturbance on ultrasonic backscatter from blood, *J. Acoust. Soc. Am.*, 75 (1984) 1265-1272.

16 Toubal M., Asmani M., Radziszewski E. and Nongaillard B., Acoustic measurement of compressibility and thermal expansion coefficient of erythrocytes, *Phys. Med. Biol*., 44 (1999) 1277-1287.

17 Tabulated data from various sources complied by Prahl S, Available: http://omlc.ogi.edu/spectra. Accessed 2010 Mar.

18 Karpiouk A. B., Aglyamov S. R., Mallidi S., Shah J., Scott W. G., Rubin J. M. and Emelianov S. Y., Combined ultrasound and photoacoustic imaging to detect and stage deep vein thrombosis: Phantom and *ex vivo* studies, *J. Biomed. Opt*., 13 (2008) 054061